Journal of Polymers and the Environment (2021) 29:1963–1977
https://doi.org/10.1007/s10924-020-02016-y

ORIGINAL PAPER

Simultaneous Removal of Cationic and Anionic Dyes from Binary Solutions Using Carboxymethyl Chitosan Based IPN Type Resin

Serkan Emik[1] · **Selin Işık**[1] · **Eren Yıldırım**[1]

Accepted: 14 December 2020 / Published online: 3 January 2021

Abstract

In this study, a novel bead form IPN type resin comprising poly (2-Dimethylaminoethyl) methacrylate and carboxymethyl chitosan networks with a high dye adsorption capacity. The adsorbent was synthesized by a combination of serial reactions, including bead formation, cross-linking, and carboxymethylation of chitosan, then the photo-polymerization of DMAEM inside these beads. To assess the simultaneous basic and acidic dye removal efficacy (Safranine T; ST and Indigo carmine; IC) and characteristics, batch adsorption experiments were carried out. The effects of different parameters such as contact time, adsorbent dosage, initial dye concentration (25–400 ppm), and pH on the adsorption process were investigated. Under optimized conditions (adsorbent dosage, 1.5 g/L; pH, 3; initial concentration 250 ppm (125 ppm ST + 125 ppm IC), temperature, 25 °C), adsorption studies showed that the resin has significant high adsorption capacity (q_e = 126 and 130.5 mg/g for ST and IC, respectively). Adsorption isotherm studies showed that Langmuir, Langmuir–Freundlich, Redlich-Peterson, and D-R models fitted the adsorption equilibrium data quite well, while the Freundlich model gave poor fittings. Besides, for all initial dye concentrations in the range of 25–400 ppm in the binary mixture (except 12.5 ppm IC initial concentration), the process is favorable. According to adsorption model calculations, the adsorption takes place with a monolayer coverage, and the main dominant force for the system is weak interactions indicating physical adsorption. Kinetics studies showed that for both dye, the adsorption process could be expressed very well by the PFO model and PSO; however, the PFO model is somewhat better in predicting the experimental q_e values.

Keywords Acidic dye removal · Basic dye removal · Adsorption · Adsorption isotherms · Adsorption kinetic · Carboxymethyl chitosan · IPN type adsorbent

Introduction

As a critical environmental pollution type, discharging of colored substances that produced by textile industries and other dyeing industries such as paper, printing, leather, food, and plastic, into water bodies not only can aesthetically cause issues but also it is harmful to biological organisms and ecology [1–5]. The presence of dyes in textile wastewater is an environmental problem due to their high visibility, resistance, and toxic nature; even deficient concentrations of dyes in water are easily visible and can reduce photosynthetic activities in aquatic environments by preventing the penetration of light and oxygen. Dyes are non-biodegradable substances that remain stable under different conditions, have direct and indirect toxic effects on humans as they are associated with cancer, jaundice, tumors, skin irritation, allergies, heart defects, and mutations [3, 5–7]. Because of these harmful effects, wastewater containing dyes are treated by such as ion exchange, coagulation/flocculation, chemical precipitation, electrochemical reaction, electrodialysis, reverse osmosis, and membrane filtration [7–14] to remove trace amounts of pollutants from wastewaters. Adsorption, as a physicochemical treatment process, has attracted

Supplementary information The online version of this article (https://doi.org/10.1007/s10924-020-02016-y) contains supplementary material, which is available to authorized users.

✉ Serkan Emik
s.emik@istanbul.edu.tr

Selin Işık
sselinsk@gmail.com

Eren Yıldırım
erenyildirim@istanbul.edu.tr

[1] Chemical Engineering Department, Faculty of Engineering, Istanbul University - Cerrahpasa, Avcılar, 34320 Istanbul, Turkey

considerable attention because it is rapid, convenient, and difficult to toxic contaminants. It also has low initial costs, in this respect, since a well-designed adsorption system can produce an effluent with virtually no dyestuffs present[15].

In wastewater treatment processes by adsorption, both organic and inorganic materials such as activated carbon, alumina, zeolites, industrial by-products, agricultural solid wastes, clays, peat, and polysaccharides [6, 16–32] have been focused on in several studies. Among these adsorbents, natural and synthetic adsorbents are found to be very effective adsorbents because of their large surface area and high adsorption capacity, suitable pore size and volume, easy accessibility, cost-effectiveness, mechanical stability, compatibility, ease of regeneration, etc.[14]. In the case of polymeric adsorbents, interpenetrating polymer networks (IPNs), principally a mixture of two or more cross-linked polymers, have gained increasing attention in adsorption processes to their extraordinary properties than those of conventional polymeric adsorbents. IPNs generally show better morphological and thermal properties, faster adsorption kinetics and response rate, and higher adsorption capacity than those formed by random copolymerization of the relevant two monomers. This case caused a great deal of attention in using them for dye and heavy metal removal from wastewaters [14]. Besides, in recent years natural polymer-based adsorbents such as starch, cellulose, and chitosan are preferred in adsorption processes due to their cost-effectiveness and environmentally friendly properties. Chitosan is an amino-based polysaccharide (poly-β-(1 → 4)-2-amino-2-deoxy-D-glucose) and produced by *N*-deacetylation of chitin (1–3 Chitin (poly-β-(1 → 4)-*N*-acetyl-D-glucosamine). Because of its great adsorption potential, numerous papers have already been published focusing of its usage as an adsorbent for the decontamination of wastewater (or effluents, seawater, drinking samples etc.) from various pollutants, either organic (dyes, phenolic and pharmaceutical compounds, herbicides, pesticides, drugs etc.) or inorganic species (metals, ions etc.). As stated in detail in two comprehensive reviews chitosan based adsorbents (e.g. IPN, Semi-IPN, derivatives with superior properties, and functional group grafted types) are used effectively and extensively for dye removal from waste water [7, 33].

Although the real possibility that different dyes (cationic, anionic, and neutral) to be present together [34, 35] in many industrial effluents, in most studies, generally, single dye solutions were studied. Considering the coexistence of different dyes in dyeing wastewater reality, the study of simultaneous adsorption of binary dyes is of great interest [36–45]. In binary dye mixtures, especially the difference in the electronegativity and polarity makes their simultaneous removal challenging. Again, adsorption was found to be one of the most efficient processes. Therefore, the prediction and evaluation of the multicomponent dye systems are still the most challenging, and it is crucial to develop a versatile adsorbent for effective simultaneous removal of different dyes[34, 43, 44].

For developing an effective process for simultaneous dye removal, most of the researchers focused on optimizing the removal efficiency by investigating the effect of process parameters such as adsorbent dosage, pH, initial concentration, etc. Some of the most recent simultaneous dye removal studies are summarized in Table 1. As it is seen from the table, depending on the type of dyes in the medium, adsorbents like activated carbon, polymer-coated magnetic particles, polymeric networks with amino, carboxyl, etc. groups were used, and removal studies were carried out in a wide range such as pH 3–12. Besides, chemical modification of chitosan with carboxyl and amino moieties was found to be one of the simplest ways to obtain an effective adsorbent for dye removal. According to literature knowledge, the adsorption capacity of this kind of adsorbent is varied between 35 and 1653 mg dye/g adsorbent depending on initial dye concentration and adsorbent's physical and chemical properties [7].

In a limited number of studies, the adsorption properties of chitosan-based adsorbents have been studied in detail. As far as we know, there is no detailed study on carboxymethyl chitosan-based IPN type adsorbent with amino functional groups. Besides, no studies have been reported about the simultaneous removal of cationic and anionic dyes. Therefore, this study aims to synthesize a novel IPN type chelating resin comprising poly (2-Dimethylaminoethyl) methacrylate and carboxymethyl chitosan networks with a high dye adsorption capacity (Safranin T and Indigo Carmine) and investigate its potential use for dye removal from single and binary aqueous solutions.

Experimental

Materials

Low molecular weight chitosan (Ch), (2-Dimethylaminoethyl) methacrylate (DMAEM), glutaraldehyde solution (25% in water) (GLA), ethylene glycol dimethacrylate (EGDM), monochloroacetic acid, dyes "Safranine T" (ST) and "Indigo carmine" (IC) were all purchased from Sigma Aldrich Co (USA). The photo-initiator 2-Hydroxy-4′-(2-hydroxyethoxy)-2-methylpropiophenone (PI) was also purchased from Sigma-Aldrich Co and used as received. The rest of the materials were analytical grade and used as received.

Table 1 Comparison of dye adsorption capacity of various adsorbents in binary solutions

Adsorbent	Dyes	Optimum Conditions	Qmax (mg/g)	Refs
Cobalt ferrite-alginate	Reactive red 195 (RR) Reactive yellow 145 (RY)	pH 3–6 Concentration: 5–130 ppm Adsorbent dosage: 10 g/L	RR: 6.5 RY: 4.2	[44]
Polyaniline@SiO2	Titan yellow (TY) Bromophenol (BP)	pH 3 Concentration: 202 mg/L for BP, 218 mg/L for TY Adsorbent dosage: 4.8 g/L	TY: 141.5 BP: 129.6	[36]
Zirconium-based metal organic frameworks loaded on polyurethane foam	Neutrally charged Rhodamine B (RB) Positively charged methylene blue (MB) Negatively charged Congo red (CR)	pH 3 Concentration: 5–30 mg/L Flow rate: 1 mL/h	Removal Efficiency: 95.73%	[37]
Amphoteric β-cyclodextrin-based adsorbent	bisphenol A, (BPA), cationic dye (methylene blue, MB) and anionic dye (methyl orange, MO)	pH 6.5 for BPA, 4 for MO, and 11 for MB Concentration: 25–500 ppm Adsorbent dosage: 1 g/L	MO: 165.8 MB: 335.5 BPA: 79	[34]
Activated carbon	Indigo carmine (IC) Methylene blue (MB)	Concentration: 50–300 ppm Adsorbent dosage: 12.5–37.5 g/L	IC: 31.02 MB:57.35	[46]
Vitis tree leaves powder	Alizarin red (AR) Methylene blue (MB)	pH 3.0, Concentration: 999.6 ppm for AR and 878.5 ppm for MB Adsorbent dosage: 5 g/L	AR: 54.6 MB: 43.9	[41]
pMMA/ Fe3O4 nanoparticles	Brilliant green (BG) Malachite green (MG)	pH 4–10, optimum 8 Concentration: 50–1500 ppm Adsorbent dosage: 8 g/L;	BG: 5.7 to 56.2 MG: 6.1 to 65.6	[42]
Activated carbon	Indigo carmine (IC)	pH 3.0, Concentration: 100–500 ppm Adsorbent dosage: 4 g/L	140 mg/g	[47]
Chitosan/Cellulose Beads	Methylene Blue (MB) Congo Red (CR)	pH 6.5 Concentration: 5 and 80 µM (1.5 to 25 ppm for MB, 3.5 to 56 ppm for CR) Adsorbent dosage: 10 g/L	CR: 1115 MB: 216	[35]

Synthesis and Characterization of the IPN Type Adsorbent

The synthesis procedure of the IPN type adsorbent is illustrated in Fig. 1, and the detailed synthesis procedure is given in the Supplementary File. Briefly, the four main steps of the synthesis procedure are (i) Preparation of Ch beads: The chitosan spheres were prepared by dropping an acetic acid aqueous chitosan solution through a syringe into a gently stirred 5% NaOH solution at 70 °C. Subsequently, the formed spheres were transferred into an ethanol-NaOH solution and held for 24 h; then, they were rinsed with distilled water and air-dried for further use. (ii) Cross-linking of Ch beads: The cross-linking reaction of chitosan beads obtained in the previous step was carried out in aqueous glutaraldehyde (GLA) solution for 24 h at 40 °C. After the reaction period, the obtained beads were filtered off and washed several times with ethanol, followed by water. (iii) Modification of the cross-linked Ch beads with monochloroacetic acid to obtain cross-linked N, O-carboxymethyl chitosan beads (CMCh). (iv) The impregnation of DMAEM and EGDM acrylic monomers into the CMCh and photo-polymerization process; formation of the final form of the adsorbent.

Adsorption Studies

Adsorption experiments, including pH effect, adsorbent dosage, kinetic and isotherm studies, were evaluated in the batch method. Three 1000 ppm stock solutions of ST, IC, and ST-IC binary solutions were prepared by dissolving the desired amount of dyes in distilled water. By diluting these solutions, seven different single and binary dye solutions were prepared in a range of 25–400 ppm. For the binary component systems, all solutions were prepared at equal mass concentrations of both dyes (e.g. 400 ppm binary solution includes 200 ppm ST and 200 ppm IC). All adsorption studies were performed in 100 ml solutions under magnetic stirring (100 rpm, 25 °C) for three runs, and the average of the adsorption data was reported.

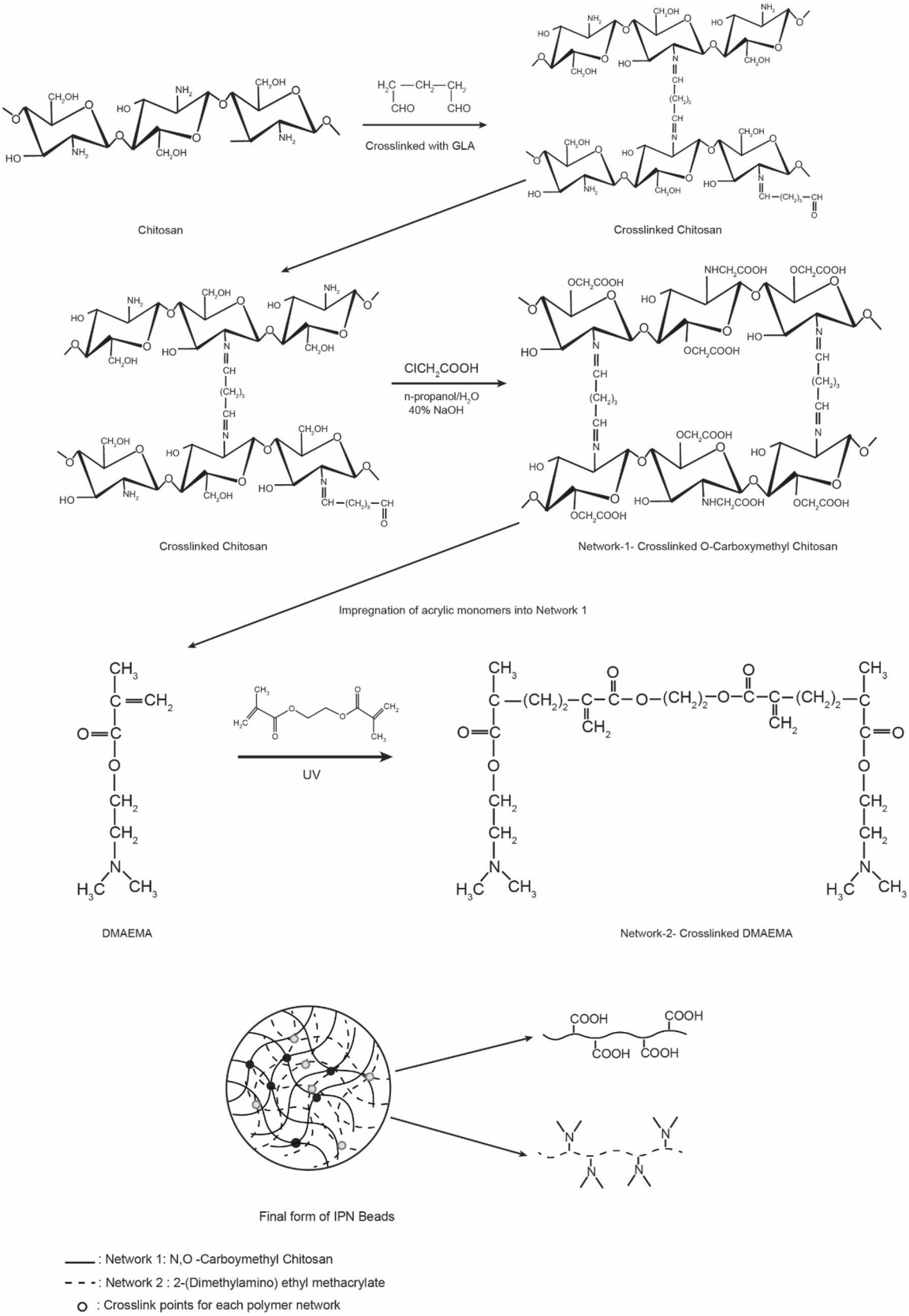

Fig. 1 Synthesis procedure and the chemical structure of the adsorbent

In adsorption experiments for single dye solutions, the residual dye concentration was monitored by a UV–VIS spectrophotometer at wavelength 522 nm for ST and 610 nm for IC. As it is seen from Figure S1, UV–VIS spectra of binary solutions at different concentrations, the 522 and 610 nm peaks are still identical, and the calibration curves give high R2 values (> 0.99). Generally, in simultaneous adsorption studies of two or more dyes in the same sample, a classic analytical problem is encountered in determining the amounts of dyes by the UV–VIS method due to the formation of the overlapped signals. It is reported that using derivative spectrophotometry in the UV–Vis region is an efficient method for simultaneous determination by increasing the spectral resolution of overlapped signals and eliminating background caused by other components or sample matrix [36, 43]. However, in this study, the UV–VIS spectra of binary mixtures show two identical peaks at 522 and 610 nm. Furthermore, no interactions were recorded for any concentration. Thus, the absorbencies at these wavelengths could able to be directly used for residual dye concentration calculations.

The adsorption capacity of the adsorbent was calculated as follows:

$$q_e = \frac{\left(C_i - C_e\right)xV}{\mathrm{m}} \quad (1)$$

where q_e is the adsorption capacity of the adsorbent (mg g^{-1} or mol g^{-1}), C_i is the initial concentration of dye (mg L^{-1} or mol L^{-1}), C_e is the final concentration of dye in the solution (mg L^{-1} or mol L^{-1}), m is the weight of adsorbent (g), and V is the volume of the solution (L). In kinetic studies calculations, q_e and C_e *were* given as q_t and C_t, which represent the adsorption capacity and dye concentration for a given time, respectively.

The Eq. 2 was also used for investigating the removal efficiency (RE %) of the adsorbent.

$$RE\% = \frac{\text{Initial dye concentration} - \text{Dye concentration after adsorption}}{\text{Initial dye concentration}} x100 \quad (2)$$

As a result of preliminary studies to determine some crucial parameters such as adsorbent dosage, pH, and contact time; the adsorbent dosage, pH, and time to reach total equilibrium for ST and IC single and binary dye solutions were decided to be 1.5 g/L, pH 3 and 72 h, respectively.

Kinetic studies were also performed at 25 °C, and the initial dye concentration, pH, and adsorbent dosage parameters were chosen 250 ppm, pH 3 (for ST single solution pH was chosen 3 and 7), and 1.5 g/L, respectively.

To evaluate the adsorption isotherms, a series of adsorption studies were performed by varying the initial dye concentration in the range of (25–400 ppm) at pH 3. The adsorption time was extended to 72 h in these experiments to achieve adsorption equilibrium.

Desorption and Reusing Studies

Desorption of dyes adsorbed on the resin was performed by contacting 0.1 g dye adsorbed- IPN-CCh sample and 10 mL 0.1 M NaOH solution with 200 rpm mixing speed at room temperature for 2 h, then 10 mL 0.1 M HCl for another 2 h. Thereafter the IPN-CCh sample was washed with distilled water and dried in a vacuum oven for the next cycle of adsorption. To determine the reusability of the hydrogels, consecutive adsorption–desorption cycles were repeated three times by using the same resin sample.

Instruments

The photo-polymerization reaction was carried out in a Pro-Ser Testing Technologies UV irradiation chamber (Istanbul-Turkey), which had an interior footprint of 60 × 40 cm, a height of 27 cm equipped with a 300 W UV-C source.

The FT-IR spectra measurements were carried out by an Agilent Cary 630 (USA) model FT-IR spectrophotometer using the KBr pellets with a dilution of 1:200.

In the dye adsorption experiments, pH values of the aqueous solutions were measured by a Hanna HI221 model pH meter (USA), and the dye concentration was measured by a PG Instruments T80 model UV–VIS spectrophotometer (UK).

Results and Discussion

Adsorbent Dosage and Effect of pH

In terms of economic effects, determining the optimum adsorbent dosage in adsorption processes is a crucial issue; hence, in this study, firstly, optimum adsorbent dosage at different pH was determined. The adsorbent dosage was chosen 1.5 g/L for both single and binary dye solutions according to preliminary adsorbent dosage studies performed for single dye solutions (results not given).

In the case of pH effect studies for single dye systems given in Fig. 2, it was determined that IC dye could be adsorbed when the solution pH is below 3 while ST could be adsorbed in the range of pH 3–10. At pH 3, the absorption capacity, qe, was found to be 165 and 160 mg/g for ST and IC, respectively.

As it is given schematically in Fig. 3, while the electrical charges of adsorbent active sites "–NH_2 /–COOH" are NH_2^+

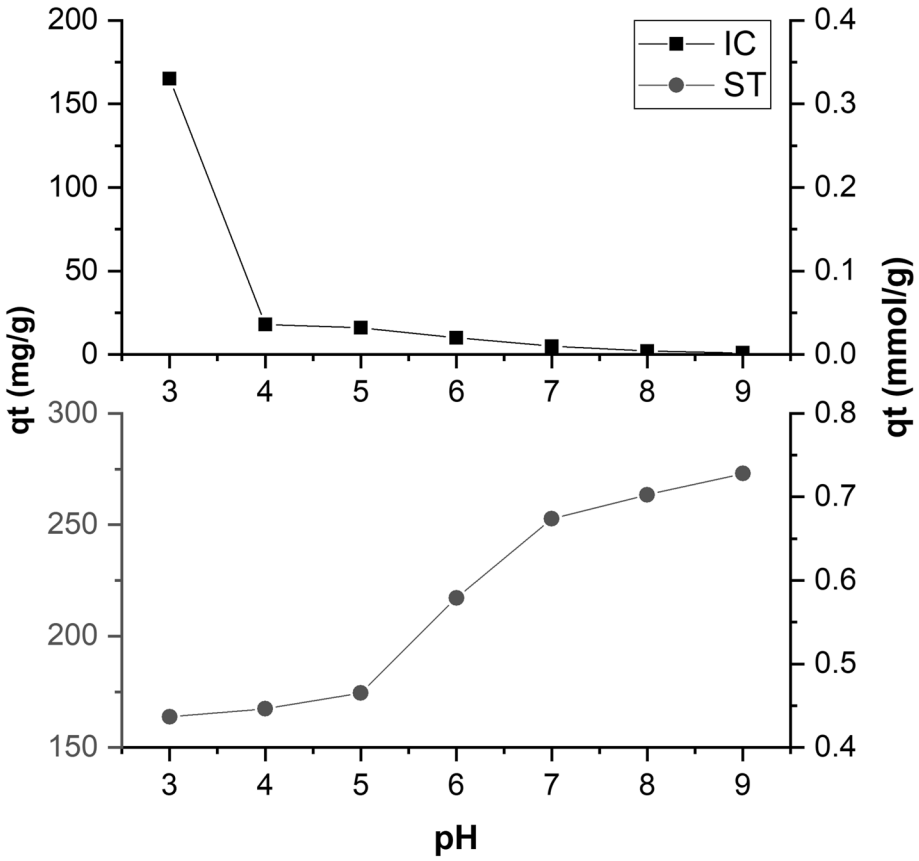

Fig. 2 pH effect on the adsorption for ST and IC single-dye systems. Adsorbent dosage: 1.5 g/L, t = 72 h, T = 25 °C, stirring speed = 100 rpm, C_0 = 250 mg/L

/ COO^- at intermediate pH; they are "NH_2^+ /–COOH", and "NH_2/COO^- " at lower and higher pH, respectively. Also, both dyes behave similarly depending on pH, and the electrical charge of the molecules changes depending on the pH.

In the case of ST adsorption from a single dye solution, in the pH 3–10 region, it can be expressed obviously that the higher the pH, the higher the COO^- groups of the adsorbent, which also provide electrostatic interactions with N^+ groups of the dye molecule. Besides that, there is considerable adsorption even at pH 3 where COOH groups are thought to be non-ionizable (protonated), which is suggesting that the ST adsorption is occurred by the electrostatic

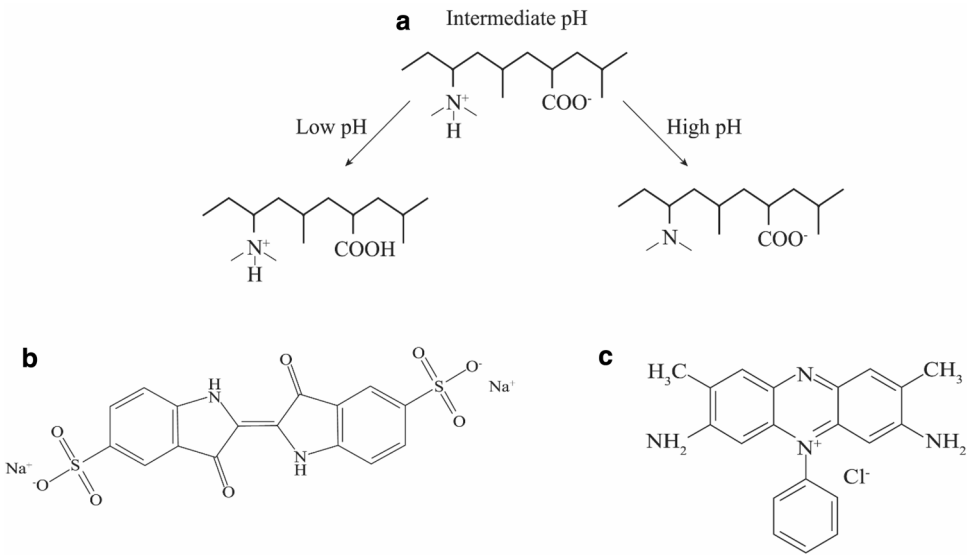

Fig. 3 Schematic illustration of **a** functional groups of IPN-CCh resin at different pHs, **b** IC, **c** ST

interactions at high pH, while the dominant mechanism at lower pHs is the π–π interactions between the dye molecule and the adsorbent[48].

Contrary, COO^- groups act as IC adsorption preventing in the pH 4–10 region due to the electrical repulsion forces; thus there is no recordable IC adsorption till pH 3. At pH 3, the NH_2 groups of the adsorbent are fully protonated. They exist as NH_2^+, which can easily interact with IC molecules, as well as the intermolecular hydrogen bonding may be an additional contributive factor.

According to these findings and conclusions, to obtain more significant information about possible competition between two dyes during the adsorption in binary solutions, pH was fixed to 3 in the kinetic and isotherm studies.

Initial Dye Concentration Effect and Adsorption Isotherms

The adsorption isotherms are one of the most critical data for comprehension of the adsorption processes. They describe the relationship between the amount of adsorbate adsorbed on the adsorbent and the dissolved adsorbate concentration in the liquid at equilibrium for a given pH and temperature. In adsorption isotherm experiments, the effect of initial dye concentration on equilibrium was investigated by carrying out adsorption experiments with the following conditions (Dosage: 1.5 g/L, pH 3, t = 72 h, T = 25 °C, stirring speed = 100 rpm, $C_0 = 25 - 400$ mg/L).

The effect of initial dye concentration on removal efficiency was represented in Table 2. As it is seen from the table, until the total dye initial concentration is 150 ppm (75 ppm ST + 75 ppmIC), the removal efficiency is relatively high for both dyes (> 75%). Since the lower the concentration, the lower the dye-adsorbent interactions, which may cause a decrease in removal; this finding indicates that the synthesized adsorbent is quite effective in the removal of ST and IC in binary solution at given conditions. Since the adsorbent was synthesized by a simple method and mostly from a biopolymer, chitosan, and has a considerably high removal capacity than those of previously reported resins have, it is concluded that the synthesized adsorbent should have advantages particularly economically.

Table 2 The removal efficiency of the adsorbent at different initial dye concentrations in binary solutions

Initial dye concentration (ppm)			Removal (%)	
Total dye	ST	IC	ST	IC
25	12.5	12.5	91	83
50	25	25	89	80
100	50	50	87	70
150	75	75	76	63
250	125	125	65	55
300	150	150	46	46
400	200	200	43	35

To obtain more explanatory information about the adsorption equilibrium, the obtained experimental data were evaluated by Langmuir (Eq. 3), Freundlich (Eq. 4), Langmuir–Freundlich (Eq. 5), Redlich-Peterson (Eq. 6), and Dubinin-Radushkevich (D-R) (Eq. 7) adsorption isotherm models [14, 49], using "mole" or "mmole (10^{-3} mol)" form of dye content. The related equations for these isotherm models are given as:

$$q_e = \frac{q_{max} K_L C_e}{1 + K_L C_e} \tag{3}$$

$$q_e = K_F C_e^{1/n} \tag{4}$$

$$q_e = \frac{q_{LFmax} K_{LF} C_e^{1/b}}{1 + K_{Lf} C_e^{1/b}} \tag{5}$$

$$q_e = \frac{A C_e}{1 + B C_e^g} \tag{6}$$

$$q_e = q_m e^{-\beta\varepsilon^2} where \varepsilon = RTln\left(1 + \frac{1}{C_e}\right) and\ E_A = (2\beta)^{-1/2} \tag{7}$$

where q_e is the adsorbed dye amount on the adsorbent at equilibrium ($molg^{-1}$), C_e the equilibrium dye concentration in solution ($molL^{-1}$), q_{max} the monolayer capacity of the adsorbent ($molg^{-1}$), K_L the Langmuir constant ($Lmol^{-1}$) and related to the free energy of adsorption, K_f the Freundlich constant, n (dimensionless) is the indicator of adsorption intensity, K_{LF} $(L/mg)^{1/b}$ is constant and b (dimensionless) is the heterogeneity constant, A (L/mole) and B (L/mole) are constants and $0 < g < 1$, β is a constant related to the mean free energy of adsorption (mol^2kJ^{-2}), q_m the theoretical saturation capacity, ε is the Polanyi potential, which is equal to $RT\ln(1 + (1/C_e))$, where R ($Jmol^{-1}\ K^{-1}$) is the gas constant, and T (K) is the absolute temperature.

The plots that obtained the non-linear curve fitting of Langmuir, Freundlich, Langmuir–Freundlich, Redlich-Peterson, and D-R isotherm models for ST and IC in binary solution were represented in Figs. 4 and 5. Besides, the constants involved with those models and the obtained correlation coefficients were listed in Table 3.

The Langmuir and Freundlich models are probably the best known and most widely applied sorption isotherms. Langmuir model assumes monolayer adsorption onto a homogenous surface where the binding sites have equal affinity and energy, and there is no transmigration or

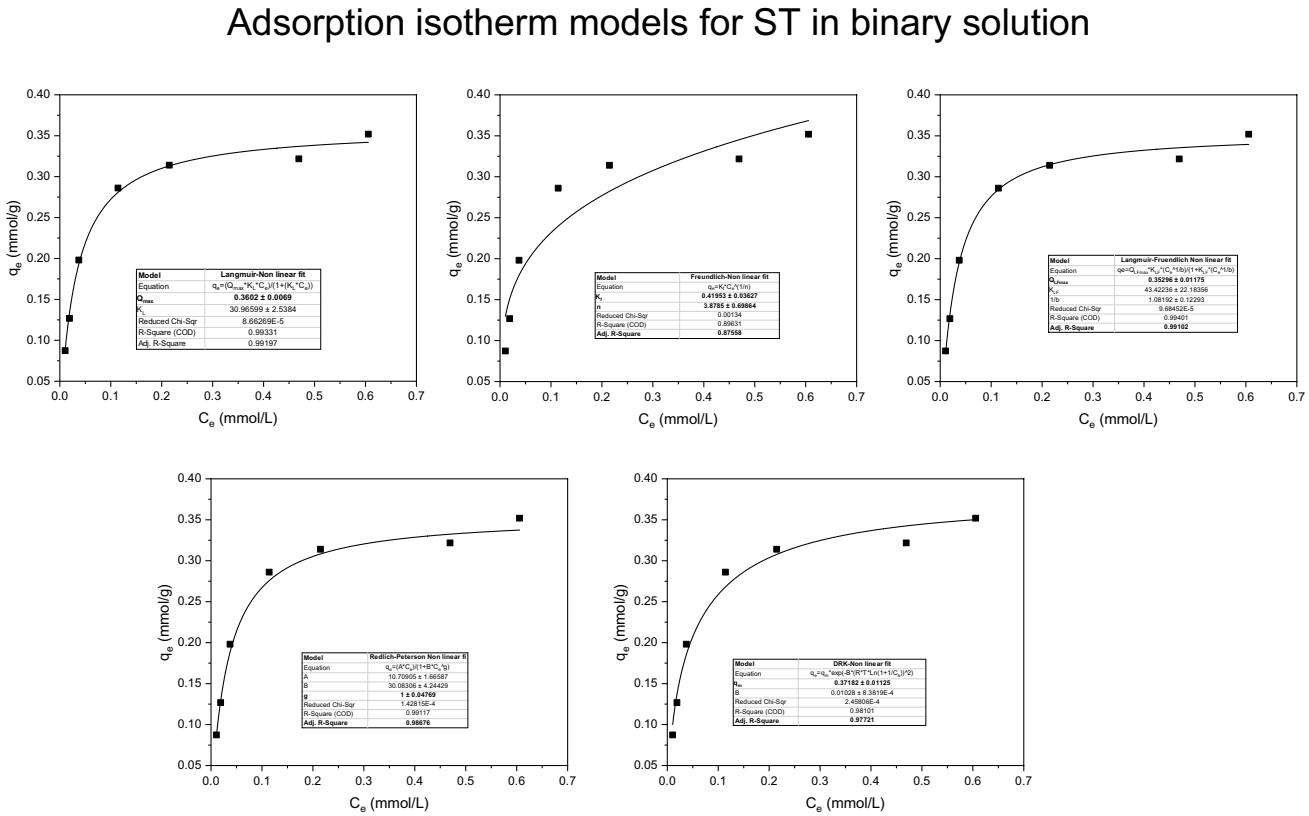

Fig. 4 Non-linear fittings of isotherm models for ST in binary solution. Adsorbent dosage: 1.5 g/L, pH 3, t = 72 h, T = 25 °C, stirring speed = 100 rpm, $C_0 = 25 - 400$ mg/L (ST concentration 12.5–200 mg/L)

interaction between the molecules. Although the Langmuir model sheds no light on the mechanistic aspects of sorption, it provides information on uptake capabilities and is capable of reflecting the usual equilibrium sorption process behavior [49, 50]. Contrarily, the Freundlich model does not indicate a finite uptake capacity of the sorbent. It assumes multilayer adsorption on the heterogeneous surface, and the amount of adsorbed adsorbate increases infinitely with an increase in concentration. Usually, by using the Redlich and Langmuir–Freundlich models together, the compatibility of adsorption to the Langmuir or Freundlich model can be explained. In general, when the Redlich model g value is 1, the system is well defined by the Langmuir model, and when it tends to 0, the system is described by the Freundlich model. Also, by using the D-R model, it is possible to have an idea about the maximum adsorption -capacity and the mean energy of the adsorption process. Besides, the favorability of the adsorption process can also be investigated by the dimensionless constant of the Langmuir model, namely separation constant, R_L, that is defined as:

$$R_L = \frac{1}{1 + K_L C_0} \tag{8}$$

where C_0 is the highest initial metal ion concentration, and the adsorption is favorable if $0 < R_L < 1$.

As it is seen from Table 3, The Langmuir isotherm model has high correlation coefficients for both dyes (0.9919 and 0.9822 for ST and IC, respectively). In contrast, the Freundlich isotherm model shows a poor-fitting ($R^2 = 0.8767$ and 0.9185 for ST and IC, respectively). This finding indicates a homogenous distribution on the IPN-CCh surface and uniform interactions with the dye molecules, probably with monolayer coverage formation. In the case of the Langmuir K_L constant values that give information about the free energy of adsorption, K_L for ST adsorption is more than twice that of IC, indicating stronger adsorption strength of ST [14, 49]. Finally, when the R_L values for ST and IC adsorption are compared, it is clearly seen that for all initial dye concentrations in the range of 25–400 ppm in the binary mixtures, the R_L values for ST adsorption in binary solution found to be between 0 and 1.0, indicate clearly favorable adsorption. For IC adsorption except for 25 ppm, the R_L values lie between 0 and 1, which are also referring to favorable adsorption of IC. However, for 12.5 ppm initial IC

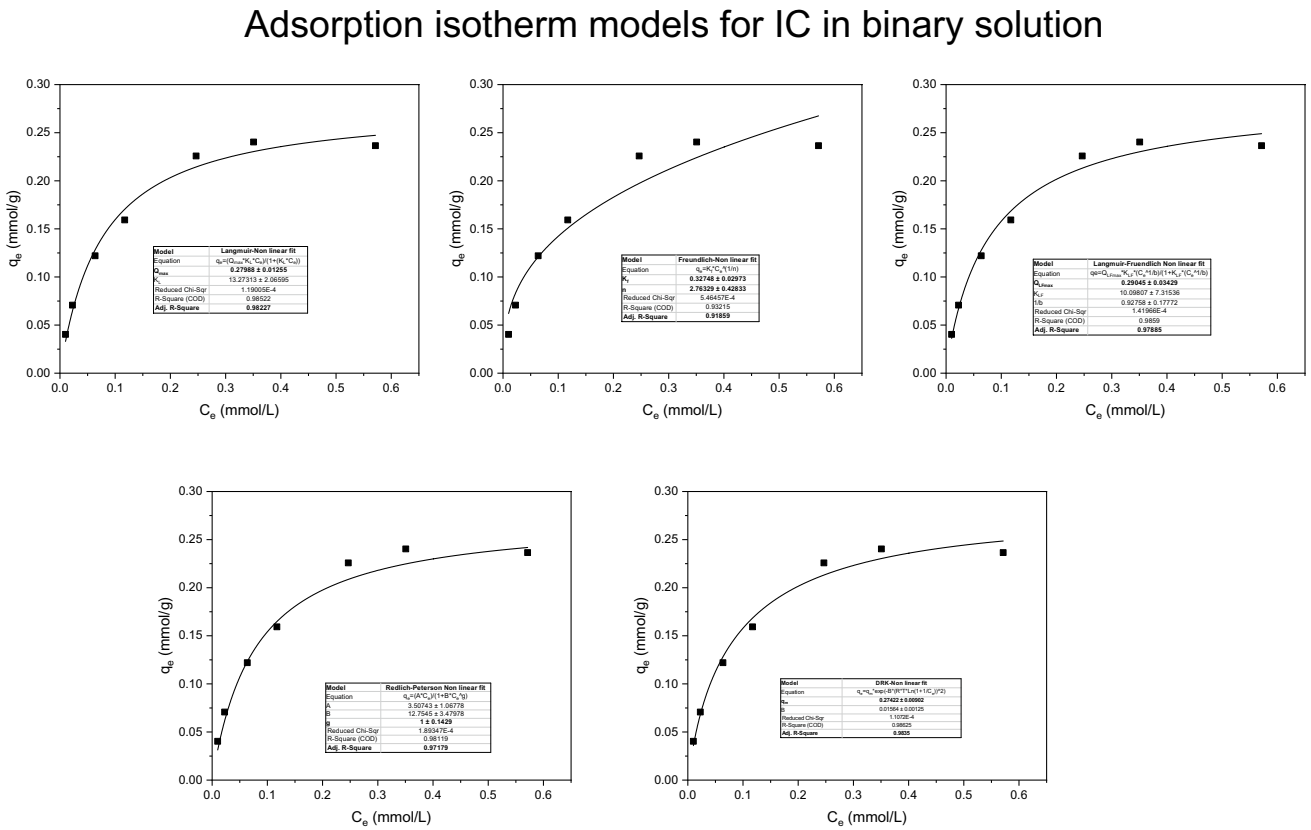

Fig. 5 Non-linear fittings of isotherm models for IC in binary solution. Adsorbent dosage: 1.5 g/L, pH 3, t = 72 h, T = 25 °C, stirring speed = 100 rpm, $C_0 = 25 - 400$ mg/L (IC concentration 12.5–200 mg/L)

concentration in 25 ppm binary dye solution, the K_L value is higher than 1. Since the RL value for IC is quite low, indicating a weak adsorption strength; hence, probably the lower the initial concentration, the weaker the adsorption is, and finally, the adsorption turns unfavorable. This case also suggests that the driving force for the adsorption of the dyes is weak interactions, i.e. van der Waals forces, π–π interactions, as well as the intermolecular hydrogen bonding as an additional contributive factor. As if confirming this situation, E_A values obtained from the D-R model ($R^2 = 0.97–0.98$) are both lower than 8 kJ/mol, which indicates physical adsorption. As it is known well, according to the dominant adsorption mechanism, the value of E_A lies in the range of 1–8, and 8–16 kJmol^{-1} [14] for physical adsorption and ion-exchange mechanism, respectively. Hence, it can be concluded that the adsorption of both dyes in binary solution occurs via physical adsorption performed through weak forces.

The maximum adsorption capacity (q_{max}) of an adsorbent is one of the most crucial property for its potential usage in separation processes. Since the Langmuir and D-R isotherm models predict the q_{max} value of an adsorbent, using these models is very useful for comparing a newly synthesized adsorbent with other adsorbents. As it is seen from Table 3, both models provide similar adsorption capacity values (~ 120–130 mg/g) for both dyes. This adsorption capacity value is considerably higher than most of the previously reported resins have[2, 34, 36, 41, 42, 44, 47].

In adsorption isotherm studies, finally, the Redlich Peterson, and Langmuir–Freundlich models were also used together for understanding if the adsorption of the dyes is compatible with the Langmuir nor Freundlich. As seen from Table 3, the Redlich Peterson g constant is equal to "1" for both dyes, indicating the process can be well-described by the Langmuir model.

According to the above conclusions, it can be said that the adsorption system for both dyes can be well-defined by Langmuir, which indicates a monolayer coverage, and the main dominant force for the system is weak interactions (e.g. van der Waals interactions between the dye molecules and the IPN-CCh surface active sites) indicating physical adsorption.

Table 3 Isotherm constants for the adsorption of ST and IC onto the resin in the binary dye solution

	Unit	ST	IC
Langmuir			
R^2		0.9919	0.9822
q_{max}	mmol/g–mg/g*	0.3602–126.4*	0.2798–130.5*
K_L	$\times 10^3$ L mol^{-1}	30.966	13.273
R_L		0.03–0.45	0.08–1.40
Freundlich			
R^2		0.8767	0.9185
N		3.8785	2.7632
K_F	$\times 10^3$ mol$^{1-1/n}$ L$^{1/n}$ g^{-1}	0.4195	0.3274
Langmuir–Freundlich			
R^2		0.9910	0.9788
$q_{LF,max}$	mmol/g–mg/g*	0.3529–123.8*	0.2904–135.4*
B		0.9243	1.0781
K_{LF}	($\times 10^3$ L/mol)$^{1/b}$	43.422	10.098
Redlich-Peterson			
R^2		0.9867	0.9717
G		1	1
A	L/mol	10.709	3.507
B	L/mol	30.083	12.754
Dubinin-Radushkevic			
R^2		0.9772	0.9835
q_m	mmol/g–mg/g*	0.3718–130.4*	0.2742–127.9*
E_A	kJmol^{-1}	6.974	5.654
B	mol^2 kJ^{-2}	0.01028	0.01564

Adsorbent dosage: 1.5 g/L, pH 3, t = 72 h, T = 25 °C, stirring speed = 100 rpm, $C_0 = 25 - 400$ mg/L

Kinetic Studies

To evaluate the adsorption kinetic properties of binary dyes on IPN-CCh, firstly, the adsorption kinetics for single dye solutions were investigated, and the obtained results were given in Figure S2. As seen from the figure, in the case of ST adsorption, the equilibrium adsorption capacity (qe) decreases from 217 to 164 mg/g (from 0.62 to 0.47 mmol/g) the pH of the solution changes from 7 to 3. Since the electrostatic interaction between IPN-CCh and ST is the leading force for the adsorption. At lower pH values, H^+ ions become competitor species for cationic dye ST and generate competitive adsorption for the same active sites; this finding is an expected situation as reported in several similar former studies[22, 51]. Besides, interestingly, significant adsorption still occurred at considerably low pH due to the fact of the possible chemical interactions (such as hydrophobic interactions, dipole–dipole interactions, etc. [52, 53].) between ST dye and IPN-CCh, which also reported in previous studies. [51, 53] In the case of IC adsorption, the adsorption capacity was found to be 160 mg/g (0.34 mmol/g), slightly lower than that of ST.

The Lagergren's pseudo-first-order kinetic (PFO) equation [54] may be written as

$$\frac{dq_t}{dt} = k_1(q_e - q_t) \tag{9}$$

The pseudo second order (PSO) kinetic rate equation [55] can be expressed as:

$$\frac{dq_t}{dt} = k_2(q_e - q_t)^2 \tag{10}$$

where q_e and q_t are the adsorption capacity at equilibrium, and at time t (mg g^{-1}) and k_1 (min^{-1}) and k_2 (g mg^{-1} min^{-1}) is the rate constant of the first and second-order adsorption model.

By integration the Eqs. (9) and (10), for the boundary conditions of $q_t = 0$ at $t = 0$ and $q_t = q_t$ at $t = t$, the equations can be transformed to the non-linear forms of kinetic models [56], which are presented as;

$$q_t = q_e(1 - e^{-k_1 t}) \tag{11}$$

$$q_t = \frac{k_2 q_e^2 \mathrm{t}}{1 + k_2 q_e t} \tag{12}$$

For single dye solutions, the kinetic data were further analyzed by the PFO and PSO kinetic models using the

non-linear curve fit function evaluated by OriginPro 2018 software. The PFO and PSO parameters for the adsorption of single dyes at pH 3 were summarized in Table 4.

The main kinetic study was performed for ST-IC 250 ppm (125 ppm ST, 125 ppm IC) binary solutions and the raw UV–VIS spectra. The graphs obtained by calculated data were given in Figure S3 and Fig. 6, respectively. From Fig. 6, it is clearly seen that qt shows a rapid increase with increasing contact time during 18 h (1080 min) and then slows down and reaches almost equilibrium value in 24 h (1440 min) for both dyes. The qe values were found to be 111 and 103 mg/g for ST and IC, respectively, which are also compatible with the values obtained from the isotherm results, and a bit lower than those of single dye systems. This finding also shows a high removal efficiency of 74 and 77% for ST and IC in binary solution.

Furthermore, another inference can be concluded that ST and IC are not in a critical competition during the adsorption process. Since ST and IC have different chemical structures and their affinities are on different adsorbent groups, this is an expected finding. Besides, it also suggests that the main forces that favor the adsorption are; hydrophobic, dipole–dipole interactions, etc., for ST and the electrostatic interactions for IC at given conditions. The formation of possible electrostatic interactions was also confirmed by FT-IR studies, which will be discussed in the next section.

To identify the controlling mechanism of adsorption, the experimental kinetic data was investigated exhaustively by the PFO and PSO kinetic models by non-linear curve fit function evaluated by OriginPro 2018 software (Fig. 7), and the parameters were summarized in Table 5.

Similar to single dye solution kinetics, for both dye solutions, it was found that the kinetics of the adsorption process could be expressed very well by the PFO model as well as PSO. However, the PFO model is somewhat better in terms of predicting the experimental q_e values.

FTIR Studies

In many adsorption processes, carboxyl and amino groups found to be having a high affinity towards the cationic and anionic dyes, respectively [21, 24, 57, 58]. Thus, in this study, a novel chitosan-based adsorbent with carboxyl and amino groups was synthesized. The N, O-carboxymethylation of chitosan, and IPN formation reactions were investigated by FTIR analysis, and the spectrum of IPN-CCh was given in Fig. 8. Since two different networks exist in the IPN structure, the characteristic IR peaks attributed to these networks can be grouped. The significant peaks for the cross-linked chitosan network can be listed as: 3350 cm^{-1} for –OH stretching vibrations; 1699 and 1614 cm^{-1} for $–NH_2$ stretching vibrations, 1020 cm^{-1} for stretching vibration of the bond C-O in polysaccharide chains. The peaks that can be attributed to the cross-linked DMAEM network can be listed as: 1719 cm-1 for carbonyl bond. These so-called peaks confirm that the synthesized IPN-CCh adsorbent has both –COOH and $–NR_2$ groups successfully synthesized.

To better understand the adsorption mechanism, the dye adsorbed IPN-CCh resin was also investigated by FT-IR and obtained spectra compared with the pure one. As it is seen from the figure, the spectrum of dye adsorbed resin showed new peaks, precise band shifts, and intensity changes due to the dye adsorption. Both dyes have phenolic ring in their chemical structures, and the formation of a new peak around 1600 cm^{-1} region confirms the dye adsorption. As it is known, IC has sulfonic acid groups in its

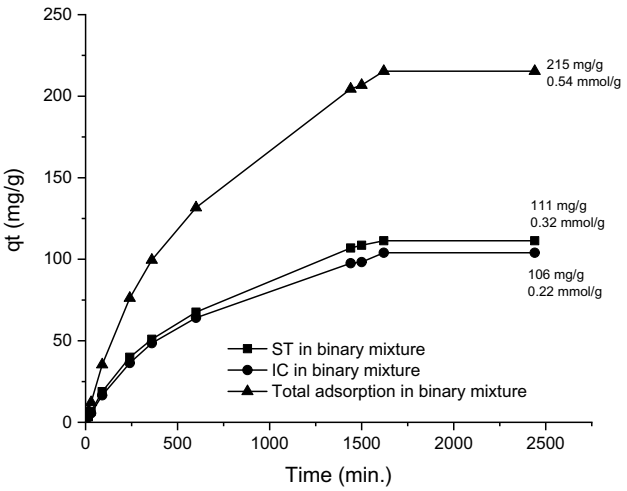

Fig. 6 Adsorption kinetics for ST and IC for the binary-dye system. Adsorbent dosage: 1.5 g/L, pH 3, T = 25 °C, stirring speed = 100 rpm, C_0 = 250 ppm (125 ppm ST + 125 ppm IC)

Table 4 Kinetic parameters for the adsorption of ST and IC onto the resin in single dye solutions

	$q_{e,exp}$	Pseudo-first-order model			Pseudo-second-order model		
		k_1	$q_{e,teo}$	r^2	k_2	$q_{e,teo}$	r^2
	(mg g^{-1})	(min^{-1})	(mg g^{-1})		(g mg^{-1} min^{-1})	(mg g^{-1})	
ST	164	0.00235	157	0.972	1.82×10^{-5}	174	0.989
IC	160	0.00251	160	0.999	1.36×10^{-5}	193	0.995

Adsorbent dosage: 1.5 g/L, pH 3, T = 25 °C, stirring speed = 100 rpm, C_0 = 250 mg/L

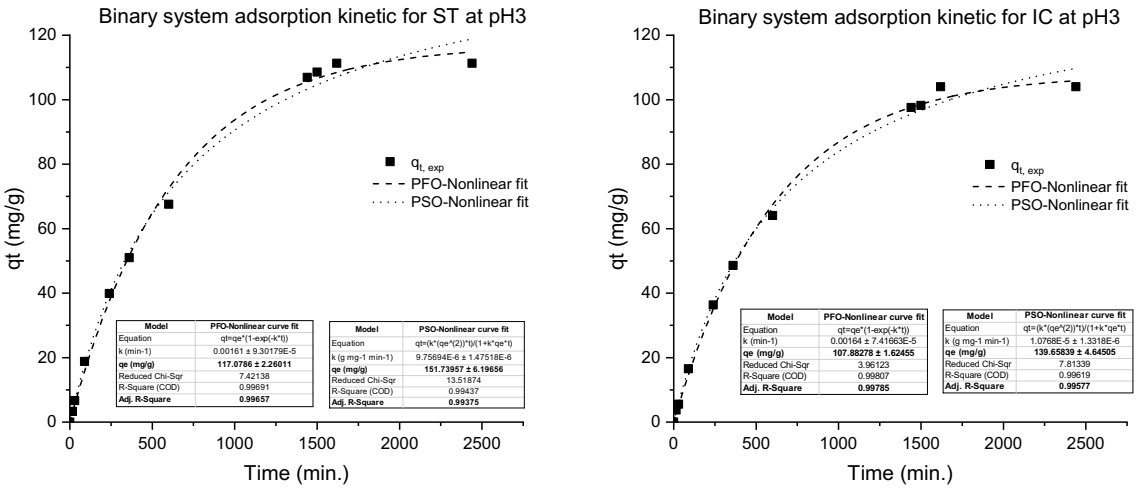

Fig. 7 Application of the PFO and PSO kinetic models for ST and IC in the binary dye solution

Table 5 Kinetic parameters for the adsorption of ST and IC onto the resin in the binary dye solution

	$q_{e,exp}$	Pseudo-first-order model			Pseudo-second-order model		
		k_1	$q_{e,teo}$	r^2	k_2	$q_{e,teo}$	r^2
	(mg g^{-1})	(min^{-1})	(mg g^{-1})		(g mg^{-1} min^{-1})	(mg g^{-1})	
ST	**117**	0.00161	117	0.996	9.75×10^{-6}	151	0.993
IC	**107**	0.00164	108	0.997	1.07×10^{-5}	139	0.996

Adsorbent dosage: 1.5 g/L, pH 3, T = 25 °C, stirring speed = 100 rpm, C_0 = 250 ppm (125 ppm ST + 125 ppm IC)

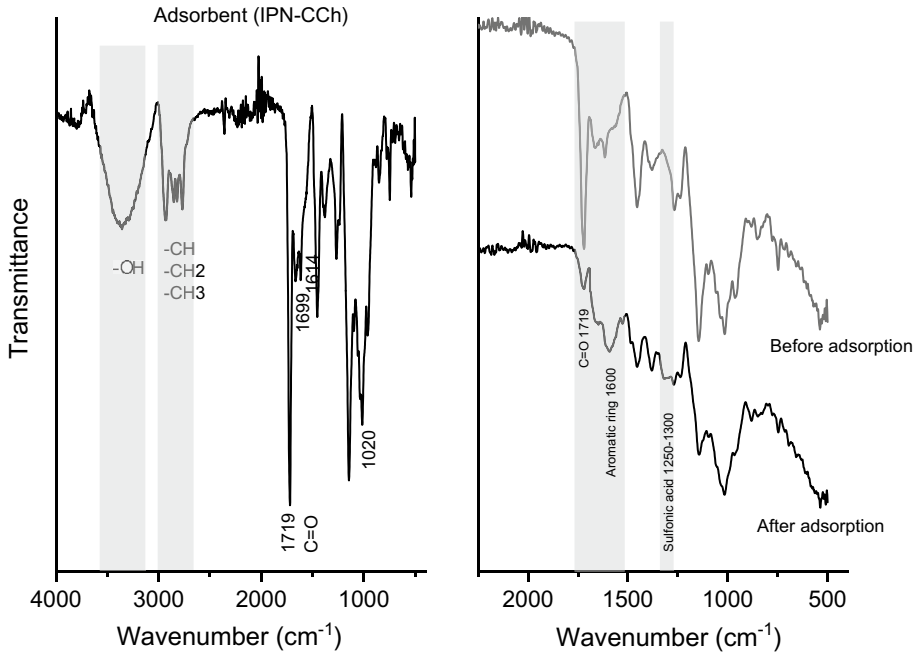

Fig. 8 FT-IR spectra of the adsorbent before and after adsorption

structure, and this group has an identical IR vibration around 1200–1300 cm^{-1}. Thus, another peak formation recorded for dye adsorbed resin at 1250–1300 cm^{-1} region confirms the adsorption of IC. Besides, the intensity of 1719 cm^{-1} band, which was attributed to the carboxyl groups of the resin, decreased dramatically after the adsorption process.

The intensity decrease is probably due to the electrostatic interactions between the carboxyl groups of the resin and the $–N^+$ groups of the dyes at given conditions. [59].

Desorption and Reusing Studies

The good desorption performance of an adsorbent and its reusability recurrently are critical parameters in its potential practical applications. According to possible adsorption mechanism, which can be directly affected by the pH of the solution and the existence of H + ions as a competitor for dyes or exchange species for the active site of the adsorbent, the regeneration process was chosen as contacting the used adsorbent samples by 0.1 M NaOH and 0.1 M HCl respectively and washing with distilled. By this process, IC and ST desorbed respectively due to the pH effect and corruption of possible electrostatic interactions between adsorbent and dye molecules by H + ions. After this regeneration process, the resin sample was dried in a vacuum oven and used two more times in the same adsorption conditions.

The obtained results showed that the adsorption capacity of the resin did not show a significant loss for both dyes at each repeated adsorption–desorption cycles. In the second and third usage, 4 and 7% loss was observed for adsorption capacity of the initial use. Thus, it can be concluded that IPN-CCh resin can be reused almost three times without a significant decrease in the adsorption capacity and recovery efficiency.

Conclusions

In this study, a novel IPN type resin comprising poly (2-Dimethylaminoethyl) methacrylate and carboxymethyl chitosan networks with a high dye adsorption capacity was synthesized. Adsorption studies showed that the resin has a significantly high adsorption capacity for both dyes. In many studies, the removal efficiencies obtained for binary solutions are relatively low compared to single solutions. However, since the synthesized adsorbent contains different active sites responsible for the adsorption of two different character dyes, the adsorption efficiency for binary solutions is very close to that of the single solutions. This case indicates that two different character dyes can be effectively removed simultaneously without showing any competition. The results showed that the synthesized IPN resin exhibited a selective adsorbent property for the removal of ST from binary mixtures at pH > 3. At the same time, it can be used as an effective adsorbent for simultaneous removal of ST and IC at pH 3. Therefore, the study can be considered to be a model study for selective and simultaneous removal of cationic and anionic organic contaminants in aqueous solutions. Once and for all, the obtained results suggest that the synthesized absorbent can be effectively used in column separation processes after the necessary process parameters optimizations are made.

Acknowledgements The authors thank Prof. Tulin Banu İyim for her assistance in the laboratory.

Author Contributions SY and EY performed the synthesis and adsorption experiments. SE managed the project studies, helped in the experimental data evolution and wrote the paper. All authors discussed the results and commented on the manuscript. The content is solely the responsibility of the authors and does not necessarily represent the official views of the İstanbul University-Cerrahpaşa Research Fund.

Funding This work was supported by the Research Fund of the Istanbul University—Cerrahpaşa; Grant Number 54352. The authors have no relevant financial or non-financial interests to disclose.

Compliance with Ethical Standards

Conflict of interest The authors have no conflicts of interest to declare that are relevant to the content of this article.

Ethical Approval All authors certify that they have no affiliations with or involvement in any organization or entity with any financial interest or non-financial interest in the subject matter or materials discussed in this manuscript.

References

1. Ceyhan O, Baybaş D (2001) Adsorption of some textile dyes by hexadecyltrimethylammonium bentonite. Turk J Chem 25:193–200
2. Gupta VK, Suhas, (2009) Application of low-cost adsorbents for dye removal: a review. J Environ Manag 90:2313
3. Crini G (2006) Non-conventional low-cost adsorbents for dye removal: a review. Bioresour Technol 97:1061–1085. https://doi.org/10.1016/j.biortech.2005.05.001
4. Ali N, Hameed A, Ahmed S (2009) Physicochemical characterization and Bioremediation perspective of textile effluent, dyes and metals by indigenous Bacteria. J Hazard Mater 164:322–328. https://doi.org/10.1016/j.jhazmat.2008.08.006
5. Buthelezi SP, Olaniran AO, Pillay B (2012) Textile dye removal from wastewater effluents using bioflocculants produced by indigenous bacterial isolates. Molecules 17:14260–14274. https://doi.org/10.3390/molecules171214260
6. Alver E, Metin AT (2012) Anionic dye removal from aqueous solutions using modified zeolite: adsorption kinetics and isotherm studies. Chem Eng J 200–202:59–67. https://doi.org/10.1016/j.cej.2012.06.038
7. Vakili M, Rafatullah M, Salamatinia B et al (2014) Application of chitosan and its derivatives as adsorbents for dye removal from water and wastewater: a review. Carbohydr Polym 113:115–130. https://doi.org/10.1016/J.CARBPOL.2014.07.007
8. Abdullah AZ, Salamatinia B, Kamaruddin AH (2009) Application of response surface methodology for the optimization of NaOH treatment on oil palm frond towards improvement in the sorption of heavy metals. Desalination 244:227–238. https://doi.org/10.1016/j.desal.2008.06.004
9. Xing Y, Chen X, Wang D (2007) Electrically regenerated ion exchange for removal and recovery of Cr(VI) from wastewater.

Environ Sci Technol 41:1439–1443. https://doi.org/10.1021/es061499l
10. Chafi M, Gourich B, Essadki AH et al (2011) Comparison of electrocoagulation using iron and aluminium electrodes with chemical coagulation for the removal of a highly soluble acid dye. Desalination 281:285–292. https://doi.org/10.1016/j.desal.2011.08.004
11. Kurniawan TA, Chan GYS, Lo W-H, Babel S (2006) Physico-chemical treatment techniques for wastewater laden with heavy metals. Chem Eng J 118:83–98. https://doi.org/10.1016/j.cej.2006.01.015
12. García-Gabaldón M, Pérez-Herranz V, García-Antón J, Guiñón JL (2006) Electrochemical recovery of tin from the activating solutions of the electroless plating of polymers. Galvanostatic operation. Sep Purif Technol 51:143–149. https://doi.org/10.1016/j.seppur.2005.12.028
13. Mohammadi T, Razmi A, Sadrzadeh M (2004) Effect of operating parameters on Pb^{2+} separation from wastewater using electrodialysis. Desalination 167:379–385. https://doi.org/10.1016/j.desal.2004.06.150
14. Emik S (2014) Preparation and characterization of an IPN type chelating resin containing amino and carboxyl groups for removal of Cu(II) from aqueous solutions. React Funct Polym 75:63–74. https://doi.org/10.1016/J.REACTFUNCTPOLYM.2013.12.006
15. Choy KKH, Porter JF, McKay G (2000) Langmuir isotherm models applied to the multicomponent sorption of acid dyes from effluent onto activated carbon. J Chem Eng Data 45:575–584. https://doi.org/10.1021/je9902894
16. Saha TK, Bhoumik NC, Karmaker S et al (2011) Adsorption characteristics of reactive black 5 from aqueous solution onto chitosan. Clean: Soil, Air, Water 39:984–993. https://doi.org/10.1002/clen.201000315
17. Güçlü G, Keleş S, Güçlü K (2006) Removal of Cu^{2+} ions from aqueous solutions by starch-graft-acrylic acid hydrogels. Polym Plast Technol Eng 45:55–59. https://doi.org/10.1080/03602550500373741
18. Güçlü G, Gürdağ G, Özgümüş S (2003) Competitive removal of heavy metal ions by cellulose graft copolymers. J Appl Polym Sci 90:2034–2039. https://doi.org/10.1002/app.12728
19. Keleş S, Güçlü G (2006) Competitive removal of heavy metal ions by starch-graft-acrylic acid copolymers. Polym Plast Technol Eng 45:365–371. https://doi.org/10.1080/03602550600553291
20. Güçlü G, Güçlü K, Keleş S (2007) Competitive removal of nickel (II), cobalt (II), and zinc (II) ions from aqueous solutions by starch-graft-acrylic acid copolymers. J Appl Polym Sci 106:1800–1805. https://doi.org/10.1002/app.26866
21. Güçlü G, Keleş S (2007) Removal of basic dyes from aqueous solutions using starch-graft-acrylic acid copolymers. J Appl Polym Sci 106:2422–2426. https://doi.org/10.1002/app.26778
22. Al E, Güclü G, Ïyim TB et al (2008) Synthesis and properties of starch-graft-acrylic acid/Na-montmorillonite superabsorbent nanocomposite hydrogels. J Appl Polym Sci 109:16–22. https://doi.org/10.1002/app.27968
23. Iyim TB, Güçlü G (2009) Removal of basic dyes from aqueous solutions using natural clay. Desalination 249:1377–1379. https://doi.org/10.1016/j.desal.2009.06.020
24. Dalaran M, Emik S, Güçlü G et al (2009) Removal of acidic dye from aqueous solutions using poly(DMAEMA-AMPS-HEMA) terpolymer/MMT nanocomposite hydrogels. Polym Bull 63:159–171. https://doi.org/10.1007/s00289-009-0077-4
25. Güçlü G, Al E, Emik S et al (2010) Removal of Cu^{2+} and Pb^{2+} ions from aqueous solutions by Starch-graft-acrylic acid/montmorillonite superabsorbent nanocomposite hydrogels. Polym Bull 65:333–346. https://doi.org/10.1007/s00289-009-0217-x
26. Guibal E, McCarrick P, Tobin JM (2003) Comparison of the sorption of anionic dyes on activated carbon and chitosan derivatives from dilute solutions. Sep Sci Technol 38:3049–3073. https://doi.org/10.1081/SS-120022586
27. Iida Y, Kozuka T, Tuziuti T, Yasui K (2004) Sonochemically enhanced adsorption and degradation of methyl orange with activated aluminas. Ultrasonics 42:635–639. https://doi.org/10.1016/j.ultras.2004.01.092
28. Bhatnagar A, Jain AK (2005) A comparative adsorption study with different industrial wastes as adsorbents for the removal of cationic dyes from water. J Colloid Interface Sci 281:49–55. https://doi.org/10.1016/j.jcis.2004.08.076
29. Wang XS, Zhou Y, Jiang Y, Sun C (2008) The removal of basic dyes from aqueous solutions using agricultural by-products. J Hazard Mater 157:374–385. https://doi.org/10.1016/j.jhazmat.2008.01.004
30. Öztürk A, Malkoc E (2014) Adsorptive potential of cationic Basic Yellow 2 (BY2) dye onto natural untreated clay (NUC) from aqueous phase: Mass transfer analysis, kinetic and equilibrium profile. Appl Surf Sci 299:105–115. https://doi.org/10.1016/j.apsusc.2014.01.193
31. Fernandes AN, Almeida CAP, Menezes CTB et al (2007) Removal of methylene blue from aqueous solution by peat. J Hazard Mater 144:412–419. https://doi.org/10.1016/j.jhazmat.2006.10.053
32. Özkahraman B, Özbaş Z (2020) Removal of Al(III) ions using gellan gum-acrylic acid double network hydrogel. J Polym Environ 28:689–698. https://doi.org/10.1007/s10924-019-01636-3
33. Kyzas GZ, Bikiaris DN, Mitropoulos AC (2017) Chitosan adsorbents for dye removal: a review. Polym Int 66:1800–1811. https://doi.org/10.1002/pi.5467
34. Zhou Y, Hu Y, Huang W et al (2018) A novel amphoteric β-cyclodextrin-based adsorbent for simultaneous removal of cationic/anionic dyes and bisphenol A. Chem Eng J 341:47–57. https://doi.org/10.1016/j.cej.2018.01.155
35. Vega-Negron AL, Alamo-Nole L, Perales-Perez O et al (2018) Simultaneous adsorption of cationic and anionic dyes by chitosan/cellulose beads for wastewaters treatment. Int J Environ Res 12:59–65. https://doi.org/10.1007/s41742-018-0066-2
36. Rastgordani M, Zolgharnein J, Mahdavi V (2020) Derivative spectrophotometry and multivariate optimization for simultaneous removal of Titan yellow and Bromophenol blue dyes using polyaniline@SiO2 nanocomposite. Microchem J 155:104717. https://doi.org/10.1016/j.microc.2020.104717
37. Li J, Gong J-L, Zeng G-M et al (2018) Zirconium-based metal organic frameworks loaded on polyurethane foam membrane for simultaneous removal of dyes with different charges. J Colloid Interface Sci 527:267–279. https://doi.org/10.1016/j.jcis.2018.05.028
38. Archin S, Sharifi SH, Asadpour G (2019) Optimization and modeling of simultaneous ultrasound-assisted adsorption of binary dyes using activated carbon from tobacco residues: response surface methodology. J Clean Prod 239:118136. https://doi.org/10.1016/j.jclepro.2019.118136
39. Abdi J, Mahmoodi NM, Vossoughi M, Alemzadeh I (2019) Synthesis of magnetic metal-organic framework nanocomposite (ZIF-8@SiO2@MnFe2O4) as a novel adsorbent for selective dye removal from multicomponent systems. Microporous Mesoporous Mater 273:177–188. https://doi.org/10.1016/j.micromeso.2018.06.040
40. Sharma K, Vyas RK, Singh K, Dalai AK (2018) Degradation of a synthetic binary dye mixture using reactive adsorption: experimental and modeling studies. J Environ Chem Eng 6:5732–5743. https://doi.org/10.1016/j.jece.2018.08.069
41. Bagtash M, Zolgharnein J (2018) Hybrid central composite design for simultaneous optimization of removal of methylene blue and alizarin red S from aqueous solutions using Vitis tree leaves. J Chemom 32:e2960. https://doi.org/10.1002/cem.2960

42. Zolgharnein J, Bagtash M, Shariatmanesh T (2015) Simultaneous removal of binary mixture of Brilliant Green and Crystal Violet using derivative spectrophotometric determination, multivariate optimization and adsorption characterization of dyes on surfactant modified nano-γ-alumina. Spectrochim Acta A Mol Biomol Spectrosc 137:1016–1028. https://doi.org/10.1016/j.saa.2014.08.115
43. Dil AA, Vafaei A, Ghaedi AM et al (2018) Multi-responses optimization of simultaneous adsorption of methylene blue and malachite green dyes in binary aqueous system onto Ni:FeO(OH)-NWs-AC using experimental design: derivative spectrophotometry method. Appl Organomet Chem 32:e4148. https://doi.org/10.1002/aoc.4148
44. Jayalakshmi R, Jeyanthi J (2019) Simultaneous removal of binary dye from textile effluent using cobalt ferrite-alginate nanocomposite: performance and mechanism. Microchem J 145:791–800. https://doi.org/10.1016/j.microc.2018.11.047
45. Bagheri AR, Ghaedi M, Asfaram A et al (2016) Modeling and optimization of simultaneous removal of ternary dyes onto copper sulfide nanoparticles loaded on activated carbon using second-derivative spectrophotometry. J Taiwan Inst Chem Eng 65:212–224. https://doi.org/10.1016/j.jtice.2016.05.004
46. Gupta TB, Lataye DH (2018) Adsorption of indigo carmine and methylene blue dye: Taguchi's design of experiment to optimize removal efficiency. Sadhana - Acad Proc Eng Sci 43:1–13. https://doi.org/10.1007/s12046-018-0931-x
47. Sumalatha B, Kumar YP, Kumar KK et al (2014) Biological and chemical sciences removal of indigo carmine from aqueous solution by using activated carbon. Res J Pharm Biol Chem 5:1–12
48. Qiu Y, Zheng Z, Zhou Z, Sheng GD (2009) Effectiveness and mechanisms of dye adsorption on a straw-based biochar. Bioresour Technol 100:5348–5351. https://doi.org/10.1016/j.biortech.2009.05.054
49. Trikkaliotis DG, Christoforidis AK, Mitropoulos AC, Kyzas GZ (2020) Adsorption of copper ions onto chitosan/poly(vinyl alcohol) beads functionalized with poly(ethylene glycol). Carbohydr Polym 234:115890. https://doi.org/10.1016/J.CARBPOL.2020.115890
50. Volesky B (2003) Sorption and biosorption. BV Sorbex, Montreal
51. Wang L, Li Q, Wang A (2010) Adsorption of cationic dye on N, O-carboxymethyl-chitosan from aqueous solutions: equilibrium, kinetics, and adsorption mechanism. Polym Bull 65:961–975. https://doi.org/10.1007/s00289-010-0363-1
52. Karadağ E, Üzüm ÖB (2012) A study on water and dye sorption capacities of novel ternary acrylamide/sodium acrylate/PEG semi IPN hydrogels. Polym Bull 68:1357–1368. https://doi.org/10.1007/s00289-011-0635-4
53. Greluk M, Hubicki Z (2013) Effect of basicity of anion exchangers and number and positions of sulfonic groups of acid dyes on dyes adsorption on macroporous anion exchangers with styrenic polymer matrix. Chem Eng J 215–216:731–739. https://doi.org/10.1016/j.cej.2012.11.051
54. Ho YS, McKay G (1998) A Comparison of chemisorption kinetic models applied to pollutant removal on various sorbents. Process Saf Environ Prot. https://doi.org/10.1205/095758298529696
55. Ho YS, McKay G (1999) Pseudo-second order model for sorption processes. Process Biochem 34:451–465. https://doi.org/10.1016/S0032-9592(98)00112-5
56. Zafar S, Khalid N, Daud M, Mirza ML (2015) Kinetic studies of the adsorption of thorium ions onto rice husk from aqueous media : linear and nonlinear approach. Nucleus 1:14–19
57. Özkahraman B, Bal A, Acar I, Güçlü G (2011) Adsorption of brilliant green from aqueous solutions onto crosslinked chitosan graft copolymers. Clean: Soil, Air, Water 39:1001–1006. https://doi.org/10.1002/clen.201000337
58. Dalaran M, Emik S, Güçlü G et al (2011) Study on a novel polyampholyte nanocomposite superabsorbent hydrogels: synthesis, characterization and investigation of removal of indigo carmine from aqueous solution. Desalination 279:170–182. https://doi.org/10.1016/j.desal.2011.06.004
59. Socrates G (2001) Infrared and Raman characteristic group frequencies. Tables and charts